ISBN: 978-3-95450-261-5 ISSN: 2673-7000 doi: 10.18429/JACoW-NAPAC2025-THYD02

COMPARISON OF PREDICTED AND MEASURED COLLECTIVE EFFECTS IN A FOURTH GENERATION STORAGE RING*

Ryan Lindberg, Argonne National Laboratory, Lemont, IL, USA

Abstract

Predicting, measuring, and mitigating collective instabilities in storage rings is important to maximize their performance. We will describe our efforts to theoretically compute and characterize collective effects during the design process, and how these continue during early operations. We then show how these predictions compare to measured collective effects at the APS-U, both with and without the harmonic cavity to lengthen the bunch.

INTRODUCTION

The Advanced Photon Source (APS) at Argonne National Laboratory recently underwent a major upgrade in which the third generation, double bend achromat lattice was replaced by a seven bend achromat with reverse bends [1]. This resulted in a reduction of the natural emittance by nearly two orders of magnitude, down to $\varepsilon_{x,0} = 42$ pm. In addition, the average operating current was doubled to 200 mA, so that the brightness for X-rays above 1 keV was increased by more than two orders of magnitude. Several other improvements were made to ensure that the brightness increase can be fully used, including upgrades to X-ray beam lines and the addition of a passive fourth harmonic cavity to lengthen the bunch [2, 3], thereby increasing the lifetime while mitigating other deleterious effects associated with a high peak current, including rf heating, intrabeam scattering, and other collective effects.

As part of our efforts to optimize performance, we spent considerable time during the design phase trying to compute and minimize collective effects. For example, all storage ring components were analyzed with electromagnetic solvers [4, 5], and the resulting impedances were then summed to form the ring impedance, as described in [6, 7]. For example, the longitudinal impedance was formed as

$$Z_{\parallel}(\omega) = \sum_{\text{elements } j} Z_{\parallel,j}(\omega), \tag{1}$$

where j labels the impedance element; for an element located at s_j where the beta function is $\beta_x(s_j)$, the β_x-weighted horizontal dipole impedance for the ring is

$$\left\langle \beta_x Z_x^D(\omega) \right\rangle = \sum_{\text{elements } j} \beta_x(s_j) Z_{x,j}^D(\omega), \tag{2}$$

with similar expressions used along the vertical y and for the quadrupolar impedance.

Early tracking simulations using the ring impedance in `elegant` [8, 9] were used to set a target chromaticity of $\xi_{x,y} \gtrsim 5$ to insure transverse stability, and to identify components that would benefit from a redesign to reduce the associated impedance. For example, extensive study of the flange gaps helped set tolerances on the inner diameter for the rf gaskets. Later tracking simulations showed a large margin for both transverse and longitudinal stability in the "high brightness" mode using 324 bunches, such that fills with 200 mA total current divided amongst $\gtrsim 108$ bunches should be completely stable. The "timing" mode of 48 bunches, on the other hand, had a transverse stability margin of just over a factor of two in current, while simulations indicated that the microwave instability would be mildly operative and inflate the energy spread from 0.135% to approximately 0.15%.

CALCULATIONS AND MEASUREMENTS BEFORE AND DURING COMMISSIONING

In addition to the early simulation efforts described above, there was significant work done before and during commissioning to predict and mitigate collective instabilities. First, the impedance model continued to evolve as the vacuum design [10, 11] matured. This effort often involved a few iterations with the engineers as they tried to simplify manufacture and installation considerations while keeping within cost constraints, all while insuring that the impedance was acceptable. While designs for the BPMs, absorbers, flanges, and most kickers and transitions were completed prior to the final design report (FDR) [12], there remained a number of unique components that had not been completed. In addition, the location of many components in the rf sectors was not yet fixed, and the transitions to small apertures that were needed to absorb synchrotron radiation were unknown.

The full design and layout of all components was not complete until just prior to the installation phase. Hence, the impedance model continued to evolve after the FDR until the dark time. We give a sense for how significant the resulting additions and changes are in Fig. 1. Panel (a) shows that the longitudinal impedance mostly changed in the low- and high-frequency range; the low-frequency changes reflect a mature understanding of the various apertures and components, while the difference observed at high frequency results largely from our decision to NEG-coat (but not activate) certain aluminum chambers to reduce the photon stimulated desorption. Panel (b) gives a sense of how the transverse impedance evolved by plotting the real part of the β-weighted horizontal dipole impedance: in addition to the low- and high-frequency contributions noted before, the additional increase of the transverse impedance is mostly due to several small aperture absorbers needed to protect sensitive components from synchrotron radiation. While these updates are significant, we emphasize that important

* Work supported by the U.S. Department of Energy, Office of Science, Office of Basic Energy Sciences, under Contract No. DE-AC02-06CH11357.

ISBN: 978-3-95450-261-5 ISSN: 2673-7000 doi: 10.18429/JACoW-NAPAC2025-THYD02

guidance was still obtained from the incomplete impedance model.

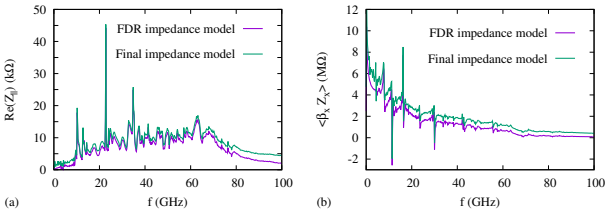

Figure 1: Evolution of the impedance during the dark time. The purple lines show the computed ring impedance as computed for the final design report (FDR), while the green adds various small apertures, updated collimator and kicker models, and similar "one-off" contributions whose design and/or location was not completed until later.

A second activity that we undertook prior to the dark time was a full characterization of the higher-order mode (HOM) spectrum of our rf cavities. This was pursued because early simulations indicated that the APS-U could be adversely affected by multi-bunch instabilities driven by HOMs. The decreased stability compared to the old APS is partly due to the smaller radiation damping, but mostly because the instability growth rates including the harmonic cavity are larger [13, 14]. Since the APS-U did not have the money, space, or commissioning time for new rf cavities, we decided to control the HOM frequencies such that they did not significantly overlap with the beam spectrum.

Simulations showed that the cavity temperature could be used to control HOM frequencies and reliably stabilize the beam, but only if we knew all the f_{HOM}'s ahead of time [16]. For this reason, concerted effort was made prior to the dark time to fully characterize the HOM mode frequencies as a function of the cavity temperature [15]. Figure 2(a) shows an example of a grow-damp measurement of one such mode, which identifies one potentially unstable mode at a particular temperature. We change f_{HOM} by changing the cavity size; e.g., the frequency shift due to thermal expansion is

$$\Delta f_{\mathrm{HOM}} = \alpha_{\mathrm{Cu}} \left(\Delta T_{\mathrm{water}} + \frac{\Delta T}{\Delta P} P_{\mathrm{cav}} \right) f_{\mathrm{HOM}}, \qquad (3)$$

where α_{Cu} is the thermal expansion coefficient of copper, $\frac{\Delta T}{\Delta P}$ is a constant that we infer from the measurements of Fig. 2(b), and $\Delta T_{\mathrm{water}}$ is the change in cooling water temperature. The last of these is specified by the operators to set all problematic f_{HOM}'s away from the beam modes.

Figure 2(c) shows all the HOMs found with beam, color coded according to the frequency family. Because these modes were carefully characterized, early commissioning could easily identify which mode(s) were being excited when multi-bunch instabilities were observed, allowing adjustment of the cavity temperature to shift f_{HOM} and stabilize the beam. Since that time, only minor adjustments have been periodically required to insure multi-bunch stability.

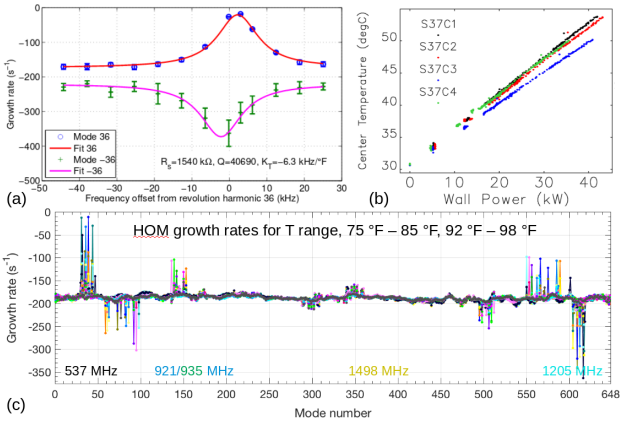

Figure 2: Higher order mode characterization for the APS rf cavities. Panel (a) shows a grow-damp measurement to identify the mode frequency and strength, while (b) plots the cavity temperature dependence on power. Panel (c) summarizes higher-order mode families and excited mode numbers.

Finally, significant work was done prior to the dark time to understand to what extent the ion instability might negatively impact the APS-U [17]. In brief, it was shown that once the vacuum became reasonably good, the ion instability only needs to be mitigated in the high-brightness mode that has 200 mA evenly distributed amongst 324 bunches. In this operation mode the relatively low-charge, closely spaced bunches can effectively trap ionized gases heavier than methane, so that we plan to break the fill into several trains separated by gaps that allow ions to escape [18, 19].

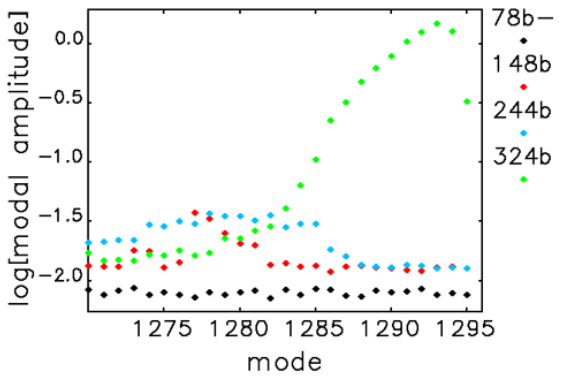

Figure 3: Evidence of the ion instability during early commissioning when the vacuum was poor. The total current is 25 mA, and the 324 bunch fill (green) shows clear signs of the ion instability. Fills with 244 (blue) and 148 (red) bunches show elevated mode oscillations, while the 78 bunch fill (black) is stable (Courtesy J. Calvey).

Present operations employ either 200 mA in a 216-bunch fill, or 140 mA in 48 bunches; neither case suffers from the ion instability, because few ions are massive enough to be trapped and because the vacuum is now quite good. During

ISBN: 978-3-95450-261-5 ISSN: 2673-7000 doi: 10.18429/JACoW-NAPAC2025-THYD02

early commissioning, however, the vacuum was rather poor and the ion instability was observed. We show evidence of the ion instability in Fig. 3, which plots the measured modal excitation for 25 mA total current divided amongst 78 bunches (black), 148 bunches (red), 244 bunches (blue), and 324 bunches (green). The 78 bunch fill is stable, while the 148 and 244 bunch fills show elevated modal amplitudes, and the 324 bunch mode shows clear signs of the ion instability. We expect similar measurements to be important if and when we employ 324 bunch fills in normal operations, particularly if we operate on the coupling (tune) resonance to make round beams with $\varepsilon_x = \varepsilon_y$.

SIMULATIONS AND MEASUREMENTS OF COLLECTIVE EFFECTS

An important prerequisite for predicting any collective effects is a good knowledge of the nominal equilibrium state. For us, this means that we need to know the longitudinal impedance sufficiently well such that the bunch length (and, ideally, bunch profile) is accurately modeled. Hence, the first item we would like to check is whether our simulations can accurately predict the single bunch current profile as a function of its current.

Unfortunately, due to time, money, and resource constraints resulting from the significant effort directed towards preparing the X-ray beamlines for operations, our streak camera is not yet fully operational (it made its first APS-U measurements in late July 2025, and should be taking data in fall of 2025). Fortunately, we have been able to use other diagnostics to extract the bunch length. For starters, some effort has been used to analyze the beam position monitor (BPM) signals to extract the bunch length. After appropriate processing, it has been found that the resulting bunch lengths are reasonably reliable, particularly for the nearly Gaussian bunches that result when the rms length $\sigma_t \lesssim 50$ ps [20, 21].

We plot comparisons between the measured (points) and simulated (lines) bunch length as a function of the single bunch current I_{bunch} in Fig. 4(a). Here, the main rf voltage is 5.225 MV and the total energy loss per turn was 3.449 MeV, and the green points are for the 324 bunch fill, while the red and blue points are for the 216 and 162 bunch fill, respectively. These should all agree with each other at fixed I_{bunch}, modulo small differences in the beam loading of the main rf cavities. Remarkably, the subtle trend observed in the simulations that fills with more bunches are slightly longer appears to also be reflected in the data.

More significantly, the agreement between the measurements and simulations is quite good up to the maximum measured bunch current of 1 mA. If we were to model the observed and simulated bunch lengthening using a purely inductive impedance by fitting it to Zotter's cubic equation [22]

$$\left(\frac{\sigma_t}{\sigma_{t0}}\right)^3 = \frac{\sigma_t}{\sigma_{t0}} + D, \tag{4}$$

we find that $D \approx 4.6 I_{\text{bunch}}[\text{mA}]$. Using the corrected factor derived in [23], we then obtain an effective ring impedance $\Im(Z_\parallel/n) \approx 0.32\ \Omega$, which is a good approximation to the low-frequency part of the simulated impedance.

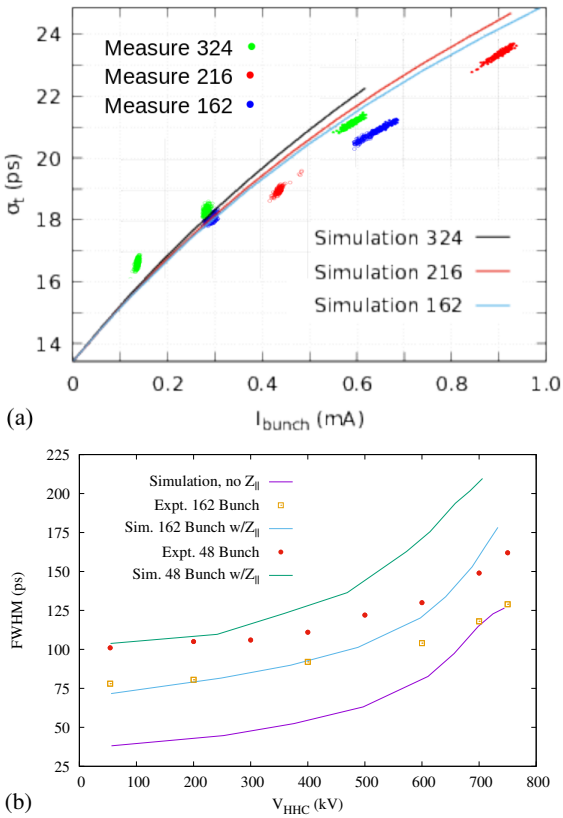

Figure 4: (a) Bunch length predictions and measurements as a function of single bunch charge for negligible harmonic voltage. (b) Bunch FWHM as a function of the harmonic cavity voltage at fixed total current of 100 mA equally distributed over either 162 or 48 bunches (b).

In addition, we would like to know how our passive, fourth-harmonic cavity affects the bunch length, as it has become an invaluable tool to lengthen the bunch and improve the lifetime. We show the results of one such study for a total ring current of 100 mA in Fig 4(b). The purple line plots the simulated bunch length as a function of the induced harmonic cavity voltage if we neglect the longitudinal impedance. This is significantly different than the measurements for both 162 bunch fills (orange squares) and the 48 bunch fill (red dots). These measurements were extracted from X-ray beamline measurements of the width of a particular atomic edge, and are therefore quoted as the full width at half maximum (FWHM).

The measured bunch length is quite close to that predicted by the simulations at low harmonic voltages, in agreement with the findings shown by Fig. 4(a). On the other hand, the simulations predict that the harmonic cavity provides more bunch-lengthening than is measured. In fact, the measurements and simulations would agree quite well if we were to reduce the measured V_{HHC} by 80%, but at this point it does not appear that such a reduction is justified by what

ISBN: 978-3-95450-261-5 ISSN: 2673-7000 doi: 10.18429/JACoW-NAPAC2025-THYD02

we measure directly from the cavity. We look forward to repeating these measurements with additional diagnostics including the streak camera, to hopefully resolve the apparent discrepancies.

The next thing that we will consider is transverse collective stability. To begin, we want to have some confidence that our impedance model accurately captures the transverse impedance that drives instability. To this end, we compare the measured tune shift with charge to that predicted by simulations in Fig. 5. Panel (a) plots the horizontal tune shift $\Delta\nu_x$ while panel (b) plots the vertical shift $\Delta\nu_y$, and each plot contains two measured data sets (in purple and green) that show good consistency. These also agree rather well with the simulated tune shift with charge when we include the full impedance in all three planes (in black). In particular, both the data and the simulations show a negative tune shift with a magnitude whose slope decreases with charge. This nonlinear behavior is primarily due to bunch lengthening from $Z_\parallel$ as shown by the orange line.

One caveat to the rather good agreement observed in Fig. 5 is that the data are restricted to the domain $0.23\,\text{mA} \lesssim I_{\text{bunch}} \lesssim 1.9\,\text{mA}$. The minimum current was set by the charge in one pulse from the linac, and we have shifted the data such that they match the simulations at 0.23 mA. The

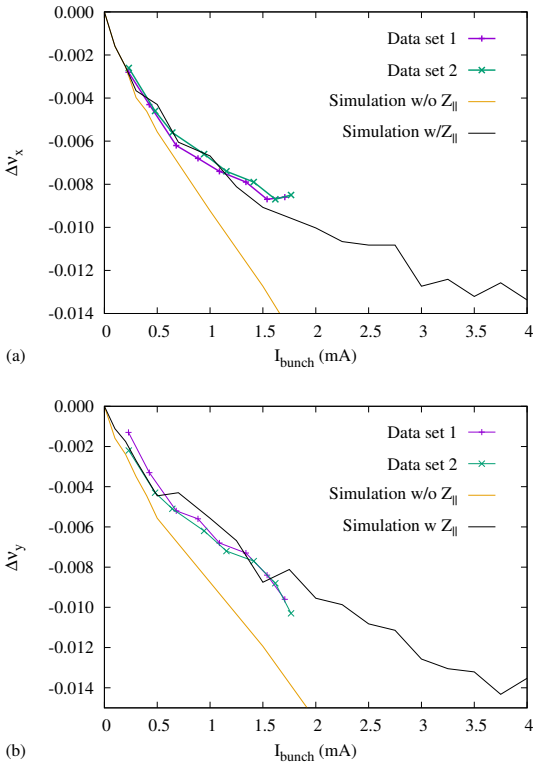

Figure 5: Comparison of the measured tune-shift-with charge to that obtained from simulations in the horizontal (a) and vertical (b) plane. Each plot has two measured data sets (in purple and green), along with simulation predictions that have no bunch lengthening due to $Z_\parallel$ (orange) and those with the simulated impedance in all planes (black).

maximum current was limited by an never-before-seen instability that appeared to have been driven by orbit correction. Future work will extend the measurements to higher and lower charges. Nevertheless, we believe that the results of Fig. 5 are quite promising.

Now that we have reasonable confidence in our transverse impedance model, the next thing we want to study is transverse collective stability. We plot the simulated predictions at $V_{\text{rf}} = 4.2$ MV for the transverse stability threshold current I_{th} as a function of the chromaticity in Fig. 6. The green and orange lines plot the horizontal and vertical current thresholds, respectively, where each is determined by setting the chromaticity ξ in the opposite plane to 5 to insure stability there, and then tracking for various bunch currents. Predictions indicate that the $\xi = 0$ threshold of about 0.28 mA can be increased above 2 mA by operating with $\xi_{x,y} \geq 3$; normal operations often has ξ_y around 3-4 with ξ_x even larger.

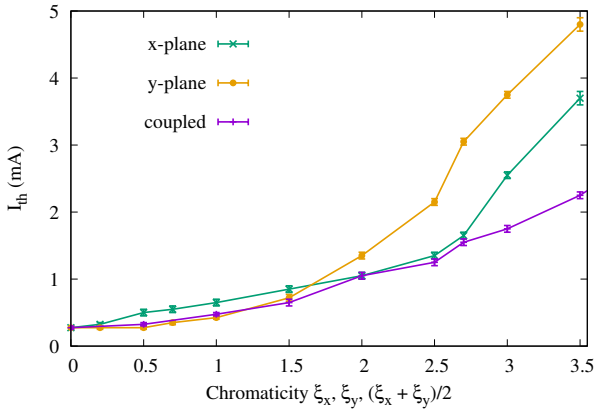

Figure 6: Simulated transverse instability limit. The x-plane limit is determined by setting $\xi_y = 5$ and varying ξ_x in an uncoupled lattice; the y-plane limit is similarly found by fixing $\xi_x = 5$ and varying ξ_y. The coupled limit uses skew quads and $\nu_x = \nu_y$ to couple the planes, fixes $\xi_y = 1$ and varies the shared chromaticity by changing ξ_x.

The purple line plots the simulated instability threshold for a coupled lattice, in which we use small values of skew quadrupoles to lightly couple the lattice, and then set $\nu_x = \nu_y$ such that the difference resonance completely couples the x and y degrees of freedom. In this case, the independent degrees of freedom have equal contributions from the horizontal and vertical motion, so that the effective impedance becomes the average of Z_x and Z_y, while the stabilizing effects of the chromaticity similarly contributes as the average $(\xi_x + \xi_y)/2$ [24, 25]. Our simulations fix $\xi_y = 1$ and only vary ξ_x, so that when $\xi_x \geq 1$ the horizontal direction effectively "shares" a part of its stabilizing chromaticity, and currents above 0.5 mA are possible. In addition, the transverse impedances are also shared, and one would naively expect the purple, coupled result to be between the uncoupled ones.

The simulations more or less agree with this intuition provided the shared chromaticity $(\xi_x + \xi_y)/2 \lesssim 2.8$, i.e.,

ISBN: 978-3-95450-261-5 ISSN: 2673-7000 doi: 10.18429/JACoW-NAPAC2025-THYD02

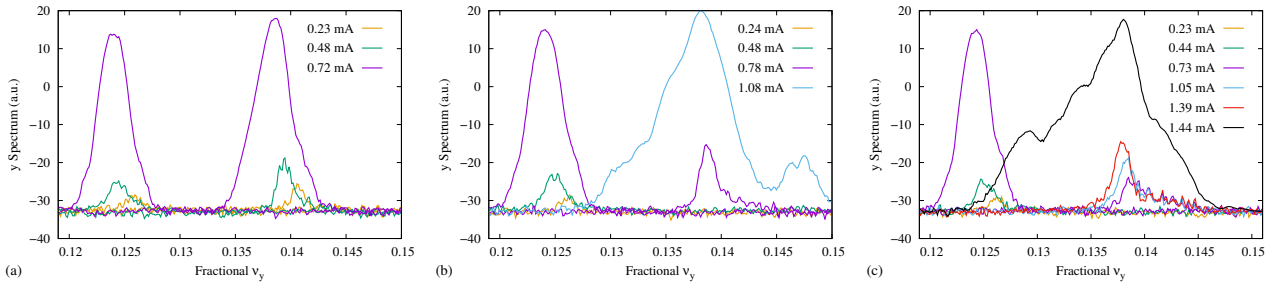

Figure 7: Spectrum measured by the Dimtel vertical pickup when $\xi_y = 1$ and $\xi_x = 3.9$ (a), $\xi_x = 4.7$ (b), and $\xi_x = 5.6$ (c). Separated tune signals are near $\nu_y \approx 0.125$, with together tune (coupled) signals are close to $\nu_y \approx 0.14$.

$\xi_x \lesssim 4.6$. Increasing ξ_x further does increase I_{th}, but not as much as one might expect from the uncoupled results. Other simulations have shown that the coupled result does lie between the two uncoupled ones if either the impedances are the same in both planes, $Z_x = Z_y$, or if we neglect the bunch lengthening due to the impedance. Hence, the somewhat unexpected findings of the coupled simulations in Fig. 6 may be related to how the bunch lengthening alters which frequencies are sampled by the impedance, but further work will be needed to verify or refute this hypothesis.

Now, we want to compare our theoretical predictions for the coupled lattice with measurements in the ring. We began with the standard user lattice and fractional tunes $\nu_x = 0.158$ and $\nu_y = 0.125$. We then tuned the skew quads such that the lattice with separated tunes remains essentially uncoupled, while knobbing the tunes together to $\nu_x = \nu_y = 0.14$ reliably provides a fully coupled beam with $\varepsilon_x = \varepsilon_y$. We set the chromaticity in both planes to $\xi_x = \xi_y = 1$, and then tested for transverse stability by increasing the injected charge and looking for evidence of bunch motion on the Dimtel vertical feedback pickup. Unfortunately, swap-out injection only allows for finite steps in charge, and for our experiment this resulted in current steps of around 0.3 mA. We considered reducing the charge per bunch by (de)tuning the injectors, but for this study we were wary of altering a highly optimized injector chain a few hours before normal user operations. In the future we will reconsider this.

Regardless, we measured a threshold current $I_{\text{th}} = 0.59 \pm 0.14$ mA when $\xi_x = \xi_y = 1$ for the uncoupled lattice with separated tunes, but a lower value of $I_{\text{th}} = 0.36 \pm 0.12$ when the tunes were together. While this is not what we expected, it is not entirely shocking given the somewhat unexpected behavior observed in the simulations. Both limits remained constant (within the measurement precision) as we increased the horizontal chromaticity until we reached $\xi_x = 3.87$, when the threshold for $\nu_x = \nu_y$ became equal to that of the uncoupled lattice. We plot the spectral measurement used to determine I_{th} for that case in Fig. 7(a).

While increasing the horizontal chromaticity did not affect the vertical stability when the tunes are separated and the motion is uncoupled, further increases to ξ_x raised the coupled (tunes together) I_{th} beyond that of the uncoupled case due to chromaticity sharing. We show our measurements at $\xi_x = 4.72$ and $\xi_x = 5.58$ in panels (b) and (c) of Fig. 7. For the highest ξ_x measured here, the instability threshold is approximately doubled.

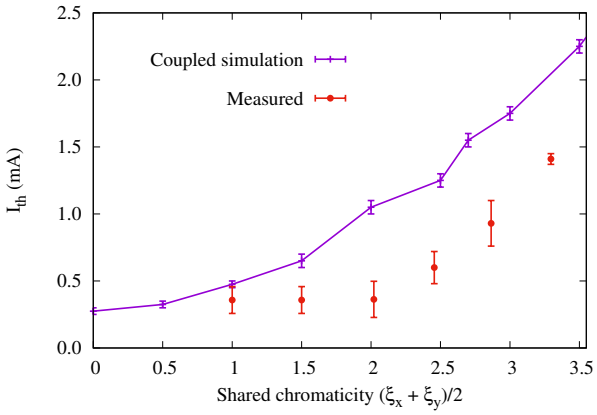

Figure 8: Comparison of the simulated and measured transverse instability limit when the tunes are brought together, the vertical chromaticity is fixed at $\xi_y = 1$, and the shared chromaticity is varied by changing ξ_x only.

Finally, we compare our measurements with the coupled tracking simulations in Fig. 8. Interestingly, the simulations and measurements approximately agree at the lowest shared chromaticity $\xi_x \approx 1$. The simulations then show a notable increase in I_{th} when the shared chromaticity increases, while the measured I_{th} doesn't change until the shared chromaticity is about 2.4 ($\xi_x \approx 3.9$). Nevertheless, the qualitative behavior is similar between the two, and importantly the shared chromaticity is shown to significantly improve stability.

ACKNOWLEDGMENTS

We thank Joe Calvey, Weixing Cheng, Louis Emery, and Sirisha Kallakuri for providing some data and figures, and thank A.J. Dick, Louis Emery, and the APS operators for help during machine studies.

REFERENCES

[1] M. Borland *et al.*, "The upgrade of the Advanced Photon Source", in *Proc. IPAC'18*, Vancouver, BC, Canada, Apr.-May 2018, pp. 2872–2877.

ISBN: 978-3-95450-261-5 ISSN: 2673-7000 doi: 10.18429/JACoW-NAPAC2025-THYD02

[2] M. P. Kelly *et al.*, "Superconducting harmonic cavity for the Advanced Photon Source upgrade", in *Proc. IPAC'15*, Richmond, VA, USA, May 2015, pp. 3267–3269. doi:10.18429/JACoW-IPAC2015-WEPTY008

[3] M. P. Kelly *et al.*, "Superconducting harmonic cavity for bunch lengthening in the APS upgrade", in *Proc. SRF'19*, Dresden, Germany, Jun.-Jul. 2019, pp. 715–717. doi:10.18429/JACoW-SRF2019-TUP102

[4] W. Bruns, http://www.gdfidl.de

[5] CST Particle Studio, http://www.3ds.com

[6] Y.-C. Chae, "The impedance database and its application to the APS storage ring", in *Proc. PAC'03*, Portland, OR, USA, May 2003, paper RPPB004, pp. 3017–3019.

[7] A. Blednykh, G. Bassi, V. Smaluk, and R. Lindberg, "Impedance modeling and its application to the analysis of the collective effects", *Phys. Rev. Accel. Beams*, vol. 24, p. 104801, 2021. doi:10.1103/PhysRevAccelBeams.24.104801

[8] M.Borland. Rep. ANL/APS LS-287, Advanced Photon Source, Argonne National Laboratory, IL, USA, 2000.

[9] Y. Wang and M. Borland, "Pelegant: A parallel accelerator simulation code for electron generation and tracking", in Proc. 12th Advanced Accelerator Concepts Workshop (AAC'6), Lake Geneva, WI, USA, Jul. 2006, *AIP Conf. Proc.*, vol. 877, p. 241–247, 2006. doi:10.1063/1.2409141

[10] B. K. Stillwell *et al.*, "Research and Development on the Storage Ring Vacuum System for the APS Upgrade Project", in *Proc. NAPAC'16*, Chicago, IL, USA, Oct. 2016, pp. 92–95. doi:10.18429/JACoW-NAPAC2016-MOPOB11

[11] J. A. Carter *et al.*, "Final Design of the APS-Upgrade Storage Ring Vacuum System", in *Proc. NAPAC'19*, Lansing, MI, USA, Sep. 2019, pp. 315–317. doi:10.18429/JACoW-NAPAC2019-TUYBB3

[12] *Advanced Photon Source Upgrade Project Final Design Report*, Argonne National Laboratory, Lemont, IL, USA, Rep. APSU-2.01-RPT-003, May 2019, https://publications.anl.gov/anlpubs/2019/07/153666.pdf

[13] L. Emery, "Required Cavity HOM deQing Calculated from Probability Estimates of Coupled Bunch Instabilities in the APS Ring", in *Proc. PAC'93*, Washington D.C., USA, Mar. 1993, pp. 3360–3363.

[14] L. Emery, T. G. Berenc, M. Borland, and R. R. Lindberg, "Multi-Bunch Stability Analysis of the Advanced Photon Source Upgrade Including the Higher-Harmonic Cavity", in *Proc. IPAC'15*, Richmond, VA, USA, May 2015, pp. 1784–1786. doi:10.18429/JACoW-IPAC2015-TUPJE065

[15] K. C. Harkay *et al.*, "Characterizing the Coupled Bunch Driving Terms in a Storage Ring", in *Proc. IBIC'17*, Grand Rapids, MI, USA, Aug. 2017, pp. 21–27. doi:10.18429/JACoW-IBIC2017-MO3AB1

[16] L. Emery, P. S. Kallakuri, D. Teytelman, and U. Wienands, "Precision Cavity Higher-Order Mode Tuning Scheme for Stabilizing the Stored Beam in the Advanced Photon Source Upgrade", in *Proc. NAPAC'19*, Lansing, MI, USA, Sep. 2019, pp. 670–672. doi:10.18429/JACoW-NAPAC2019-WEPLM04

[17] J. Calvey and M. Borland, "Simulation of incoherent ion effects in electron storage rings", *Phys. Rev. Accel. Beams*, vol. 24, p. 124401, 2021. doi:10.1103/PhysRevAccelBeams.24.124401

[18] M. Barton, "Ion trapping with asymmetric bunch filling of the NSLS VUV ring", *Nucl. Instrum. Methods in Phys. Res. A*, vol. 243, p. 278, 1986. doi:10.1016/0168-9002(86)90961-7

[19] D. Villevald and S. Heifets, "Ion trapping in the SLAC B-factory high energy ring" Rep. SLAC-TN-06-032, SLAC National Accelerfator Laboratory, Menlo Park, CA, USA, May 1993.

[20] W. Chen, Private communication, 2025.

[21] X. Sun, A. Brill, and W. Chen, paper submitted to IBIC'25, Liverpool, UK, Sep. 2025.

[22] B. W. Zotter, "Potential-well bunch lengthening" Rep. CERN SPS/81-14 (29 pages), CERN, Geneva, Switzerland, 1981.

[23] D. Zhou, G. Mitsuka, T. Ishibashi, and K. Bane, arXiv:2309.00808 [physics.acc-ph], Sep. 2023. doi:10.48550/arXiv.2309.00808

[24] E. Metral, G. Rumolo, B. Salvant, and R. R. Steerenberg, "Simulation Study of the Horizontal Head-Tail Instability Observed at Injection of the CERN Proton Synchrotron", in *Proc. PAC'07*, Albuquerque, NM, USA, Jun. 2007, paper FRPMN074, pp. 4210–4212.

[25] R. Lindberg, "Collective (In)stability Near the Coupling Resonance", in *Proc. IPAC'21*, Campinas, Brazil, May 2021, pp. 3933–3936. doi:10.18429/JACoW-IPAC2021-THPAB075